Inorg. Chem. **2006**, *45*, 1260−1269

Dioxo- and Oxovanadium(V) Complexes of Thiohydrazone ONS Donor Ligands: Synthesis, Characterization, Reactivity, and Antiamoebic Activity

Mannar R. Maurya,*,† Amit Kumar,† Abdul R. Bhat,‡ Amir Azam,‡ Cerstin Bader,§ and Dieter Rehder§

Department of Chemistry, Indian Institute of Technology Roorkee, Roorkee 247 667, India, Department of Chemistry, Jamia Milia Islamia, New Delhi 110 025, India, and Institut für Anorganische und Angewandte Chemie, Universität Hamburg, Martin-Luther-King-Platz 6, 20146 Hamburg, Germany

Received May 19, 2005

As a contribution to the development of novel vanadium complexes with pharmacologically interesting properties, two neutral dioxovanadium(V) complexes [VO_2(Hpydx-sbdt)] (**1**) and [VO_2(Hpydx-smdt)] (**3**) [H_2pydx-sbdt (**I**) and H_2pydx-smdt (**II**) are the Schiff bases derived from pyridoxal and *S*-benzyl- or *S*-methyldithiocarbazate] have been synthesized by the reaction of [VO(acac)$_2$] and the potassium salts of the ligands in methanol followed by aerial oxidation. Heating of the methanolic solutions of these complexes yields the oxo-bridged binuclear complexes [{VO(pydx-sbdt)}$_2\mu$-O] (**2**) and [{VO(pydx-smdt)}$_2\mu$-O] (**4**). The crystals and molecular structures of **1**, **3**·1.5H_2O, and **4**·2CH_3OH have been determined, confirming the ONS binding mode of the dianionic ligands in their thioenolate form. The ring nitrogen of the pyridoxal moiety is protonated in complexes **1** and **3**. Acidification of **1** and **3** with HCl dissolved in methanol afforded oxohydroxo complexes, while in a methanolic KOH solution, the corresponding dioxo species K[VO_2(pydx-sbdt/smdt)] are formed. Treatment of **1** and **3** with H_2O_2 yields (unstable) oxoperoxovanadium(V) complexes, the formation of which has been established spectrophotometrically. In vitro antiamoebic activities (against HM1:1MSS strain of *Entamoeba histolytica*) were established for all of the dioxo- and oxovanadium(V) complexes. The complexes **1**, **2**, and **4** were more effective than metronidazole, a commonly used drug against amoebiasis, suggesting that oxovanadium(V) complexes derived from thiohydrazones may open a new dimension in the therapy of amoebiasis.

Introduction

The protozoan parasite *Entamoeba histolytica* is the etiologic agent of amoebiasis, affecting millions of people worldwide, especially in tropical developing countries. Among all parasites, *E. histolytica* is the third largest killer after malaria and schistosomiasis.[1] Amoebic liver abscesses are the most frequent and severe clinical presentations of amoebiasis. Symptomatic patients typically present abdominal pain and tenderness, diarrhea, and bloody stools. Although a number of different protozoa may cause these symptoms, *E. histolytica* is the most commonly reported one. Metronidazole (MNZ) is an important drug in the treatment of several types of illnesses caused by protozoa, as well as anaerobic bacteria.[2−4] However, critical lateral effects have been described, i.e., neurological alterations produced by interaction of the drug with the central nervous system and impairment of the cardiac rhythm due to chelation of MNZ with calcium ions. MNZ also induces certain tumors in rodents and is mutagenic toward bacteria.[5−10] According to

* To whom correspondence should be addressed. E-mail: rkmanfcy@iitr.ernet.in or mannarfcy@yahoo.co.in. Tel: +91 1332 285327. Fax: +91 1332 273560.

† Indian Institute of Technology Roorkee.

‡ Jamia Milia Islamia.

§ Universität Hamburg.

(1) Schuster, H.; Chiodini, P. L. *Curr. Opin. Infect. Dis.* **2001**, *14*, 587−591.

(2) Edwards, D. I. *J. Antibiot. Chemother.* **1993**, *31*, 9−20.

(3) Lopez Nigro, M. M.; Gadano, A. B.; Carballo, M. A. *Toxicol. in Vitro* **2001**, *15*, 209−213.

(4) Moreno, S. N.; Docampo, R. *Environ. Health Perspect.* **1985**, *64*, 199−208.

(5) Akgun, Y.; Tacyldz, I.; Celik, Y. *World J. Surg.* **1999**, *123*, 102−106.

(6) Caylor, K. B.; Cassimatis, M. K. *J. Am. Anim. Hosp. Assoc.* **2001**, *37*, 258−262.

(7) Conoor, T. H.; Stoeckel, M.; Evrard, J.; Legator, M. S. *Cancer Res.* **1977**, *37*, 629−633.

10.1021/ic050811+ CCC: $33.50
Published on Web 01/04/2006

the International Agency for Research on Cancer (IARC), MNZ is classified in the 2B group, i.e., potentially carcinogenic to humans, and proved to be carcinogenic to animals.[11] This prompted us to search for new antiamoebic agents.

The transition-metal complexes of Schiff bases derived from dithiocarbazates are widely studied because of their potential for therapeutic uses[12−15] and have applications in health and skin care.[16] The coordination chemistry[17] of vanadium has acquired renewed interest since the discovery of vanadium in organisms such as certain ascidians and *Amanita* mushrooms and as a constituent of the cofactors in vanadate-dependent haloperoxidases and vanadium nitrogenase.[18] The role of vanadium complexes in catalytically conducted redox reactions,[19] potential pharmaceutical applications,[20] studies on the metabolism and detoxification of vanadium compounds under physiological conditions,[21] and the stability and speciation of vanadium complexes in biofluids[22] have also influenced the study of the coordination chemistry of vanadium. In contrast to ON donor ligands, complexes of vanadium containing sulfur functionality have not received much attention.[23] Vanadium complexes having a sulfur functionality have been found to be orally active insulin−mimetic agent in the treatment of diabetic model animals.[24] In vanadium nitrogenase, the sulfur−vanadium bond has also been well established.[25]

Scheme 1

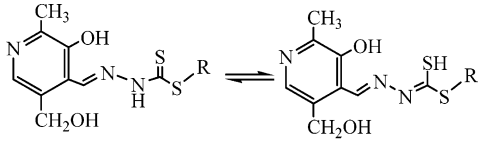

R=CH_2Ph: H_2pydx-sbdt **(I)**

R=CH_3: H_2pydx-smdt **(II)**

Recently, we have reported encouraging results on the in vitro activity of dioxovanadium(V) complexes, $[K(H_2O)_n][VO_2(X\text{-sal-sbdt})]$ (X-sal-sbdt = Schiff bases derived from salicylaldehyde and *S*-benzyldithiocarbazate, X = H, 5-Cl, 5-Br; $n = 1-2$) against *E. histolytica*.[23h] To obtain more information on the antiamoebic activity of dioxo- and oxovanadium(V) complexes with Schiff base ligands derived from *S*-benzylthiocarbazate and *S*-methylthiocarbazate, we report herein the synthesis, characterization, reactivity, and in vitro screening of the antiamoebic activity of these complexes containing the ONS donor ligands represented in Scheme 1.

(8) Kapoor, K.; Chandra, M.; Nag, D.; Paliwal, J. K.; Gupta, R. C.; Saxena, R. C. *Int. J. Clin. Pharmacol. Res.* **1999**, *19*, 83−88.
(9) Rosenkranz, H. S.; Speck, W. T. *Biochem. Biophys. Res. Commun.* **1975**, *66*, 520−525.
(10) Rowley, A.; Knight, C.; Skolimowski, M.; Edwards, D. I. *Biochem. Pharmacol.* **1980**, *29*, 2095−2098.
(11) *IARC monographs on the evaluation of the carcinogenic risk of chemicals to humans*; International Agency for Research on Cancer: Lyon, France, 1987; Supplement 7, pp 250 and 251.
(12) Klayman, D. L.; Scovill, J. P.; Bartosevitch, J. F.; Bruce, J. *J. Med. Chem.* **1983**, *26*, 35−39.
(13) Klayman, D. L. U.S. Patent 4,665,173, 1987; *Chem. Abstr.* **1987**, *107*, 115488.
(14) Pai, S. G.; Shirodkar, P. Y. *Indian Drugs* **1988**, *25*, 153−158.
(15) William, D. R. *Chem. Rev.* **1972**, *72*, 203−213.
(16) Hossain, M. E.; Alam, M. N.; Begum, J.; Ali, M. A.; Nazimuddin, M.; Smith, F. E.; Hynes, R. C. *Inorg. Chim. Acta* **1996**, *249*, 207−213.
(17) Maurya, M. R. *Coord. Chem. Rev.* **2003**, *237*, 163−181.
(18) (a) Butler, A. In *Bioinorganic Catalysis*, 2nd ed.; Reedijk, J., Bouwman, E., Eds.; Marcel Dekker: New York, 1999; Chapter 5. (b) Butler, A. *Coord. Chem. Rev.* **1999**, *187*, 17−25. (c) *Vanadium in biological systems*; Chasteen, N. D., Ed.; Kluwer Academic Publishers: Dordrecht, The Netherlands, 1990. (d) *Vanadium and its role in life [Metal ions in biological systems]*; Sigel, H., Sigel, A., Eds.; Marcel Dekker: New York, 1995; Vol. 31. (e) Messerschmidt, A.; Prade, L.; Wever, R. *Biol. Chem.* **1997**, *378*, 309−315. (f) Martinez, J. S.; Carrol, G. L.; Tschirret-Guth, R. A.; Altenhoff, G.; Little, R. D.; Butler, A. *J. Am. Chem. Soc.* **2001**, *123*, 3289−3294. (g) Robson, R. L.; Eady, R. R.; Richardson, T. H.; Miller, R. W.; Hawkins, M.; Postgate, J. R. *Nature* **1986**, *322*, 388−390. (h) Rehder, D. *J. Inorg. Biochem.* **2000**, *80*, 133−136.
(19) (a) Ligtenbarg, A. G. J.; Hage, R.; Feringa, B. L. *Coord. Chem. Rev.* **2003**, *237*, 89−101. (b) Conte, V.; Di Furia, F.; Licini, G. *Appl. Catal. A* **1997**, *157*, 335−361.
(20) (a) Pecoraro, V. L.; Slebodnick, C.; Hamstra, B. In *Vanadium Compounds: Chemistry, Biochemistry and Therapeutic Applications*; Crans, D. C., Tracy, A. S., Eds.; ACS Symposium Series; American Chemical Society: Washington, DC, 1998; Chapter 12. (b) Rehder, D. *Inorg. Chem. Commun.* **2003**, *6*, 604−617. (c) Thompson, K. H.; Orvig, C. *Met. Ions Biol. Syst.* **2004**, *41*, 221. (d) Sakurai, H.; Kojima, Y.; Yoshikawa, Y.; Kawabe, K.; Yasui, H. *Coord. Chem. Rev.* **2002**, *226*, 187−198. (e) Rehder, D.; Pessoa, J. C.; Geraldes, C. F. G. C.; Castro, M. M. C. A.; Kabanos, T.; Kiss, T.; Meier, B.; Micera, G.; Pettersson, L.; Rangel, M.; Salifoglou, A.; Turel, I.; Wang, D. *J. Biol. Inorg. Chem.* **2002**, *7*, 384−396. (f) Melchier, M.; Thompson, K. H.; Jong, J. M.; Rettig, S. J.; Shuter, E.; Yuen, V. G.; Zhou, Y.; McNeill, J. H.; Orvig, C. *Inorg. Chem.* **1999**, *38*, 2288−2293. (g) Clarke, M. J.; Zhu, F.; Frasca, D. R. *Chem. Rev.* **1999**, *99*, 2511−2533. (h) Thompson, K. H.; McNeill, J. H.; Orvig, C. *Chem. Rev.* **1999**, *99*, 2561−2571. *Trends in the use of vanadium. A report of the National Materials Advisory Board, National Academy of Science*; Publication NMAB-267; Clearinghouse for Federal Scientific and Technical Information: Springfield, VA, 1970; p 46.
(21) Baran, E. J. *J. Inorg. Biochem.* **2000**, *80*, 1−2.
(22) (a) Kiss, T.; Jakusch, T.; Pessoa, J. C.; Tomaz, I. *Coord. Chem. Rev.* **2003**, *237*, 123−133. (b) Kiss, T.; Jakusch, T.; Kilyen, M.; Kiss, E.; Lakatos, A. *Polyhedron* **2000**, *19*, 2389−2401.
(23) (a) Rehder, D. *Coord. Chem. Rev.* **1999**, *182*, 297−322. (b) Rahder, D. In *Transition Metals in Biology and Their Coordination Chemistry*; Trautwein, A. X., Ed.; Wiley-VCH: Weinheim, Germany, 1997; pp 491−504. (c) Samanta, S.; Ghosh, D.; Mukhopadhyay, S.; Endo, A.; Weakley, T. J. R.; Chaudhury, M. *Inorg. Chem.* **2003**, *42*, 1508−1517. (d) Dutta, S. K.; Samanta, S.; Kumar, S. B.; Han, O. H.; Burckel, P.; Pinkerton, A. A.; Chaudhury, M. *Inorg. Chem.* **1999**, *38*, 1982−1988. (e) Dutta, S. K.; Kumar, S. B.; Bhattacharyya, S.; Tiekink, E. R. T.; Chaudhury, M. *Inorg. Chem.* **1997**, *36*, 4954−4960. (f) Dutta, S. K.; Tiekink, E. R. T.; Chaudhury, M. *Polyhedron* **1997**, *16*, 1863−1871. (g) Maurya, M. R.; Khurana, S.; Zhang, W.; Rehder, D. *Eur. J. Inorg. Chem.* **2002**, 1749−1760. (h) Maurya, M. R.; Khurana, S.; Shailendra Azam, A.; Zhang, W.; Rehder, D. *Eur. J. Inorg. Chem.* **2003**, 1966−1973. (i) Wang, V.; Ebel, M.; Schulzke, C.; Grüning, C.; Hazari, S. K. S.; Rehder, D. *Eur. J. Inorg. Chem.* **2001**, 935−942. (j) Dutta, S. K.; Samanta, S.; Ghosh, D.; Butcher, R. J.; Chaudhury, M. *Inorg. Chem.* **2002**, *41*, 5555−5560. (k) Bhattacharyya, S.; Mukhopadhyay, S.; Samanta, S.; Weakley, T. J. R.; Chaudhury, M. *Inorg. Chem.* **2002**, *41*, 2433−2440. (l) Samanta, S.; Mukhopadhyay, S.; Mandal, D.; Butcher, R. J.; Chaudhury, M. *Inorg. Chem.* **2003**, *42*, 6284−6293. (m) Tarafder, M. T. H.; Ali, M. A.; Saravanan, N.; Weng, W. Y.; Kumar, S.; Umar-Tsafe, N.; Crouse, K. A.; Serdang, M. *Trans. Met. Chem.* **2000**, *25*, 295−298. (n) Monga, V.; Thompson, K. H.; Yuen, V. G.; Sharma, V.; Patrick, B. O.; McNeill, J. H.; Orvig, C. *Inorg. Chem.* **2005**, *44*, 2678−2688.
(24) (a) Watanabe, H.; Nakai, M.; Komazawa, K.; Sakurai, H. *J. Med. Chem.* **1994**, *37*, 876−877. (b) Sakurai, H.; Watanabe, H.; Tamura, H.; Yasui, H.; Matsushita, R.; Takada, J. *Inorg. Chim. Acta* **1998**, *283*, 175−183. (c) Sakurai, H.; Sano, H.; Takino, T.; Yasui, H. *Chem. Lett.* **1999**, 913−914. (d) Sakurai, H.; Sano, H.; Takiro, T.; Yasui, H. *J. Inorg. Biochem.* **2000**, *80*, 99−105. (e) Takeshita, S.; Kawamura, I.; Yashuno, T.; Kimura, C.; Yamamoto, T.; Seki, J.; Tamura, A.; Sakirai, H. *J. Inorg. Biochem.* **2001**, *85*, 179−186. (f) Kiss, E.; Kawabe, K.; Tamura, A.; Jakusch, T.; Sakurai, H.; Kiss, T. *J. Inorg. Biochem.* **2003**, *95*, 69−76. (g) Katoh, A.; Yamaguchi, M.; Saito, R.; Adachi, Y.; Sakurai, H. *Chem. Lett.* **2004**, *30*, 1274−1275.
(25) (a) *Biology and Biochemistry of Nitrogen Fixation*; Dilworth, J. M., Glenn, A. R., Eds.; Elsevier: Amsterdam, 1991. (b) Eady, R. R.; Legh, G. J. *J. Chem. Soc., Dalton Trans.* **1994**, 2739−2747.

Table 1. Crystal Data and Structure Refinement Parameters for **1**, **3**·2H_2O, and **4**·2CH_3OH

	1	**3**·1.5H_2O	**4**·2CH_3OH
empirical formula[a]	$C_{16}H_{16}N_3O_4S_2V$	$C_{10}H_{15}N_3O_{5.5}S_2V$	$C_{11}H_{14}N_3O_{4.5}S_2V$
fw,[a] g mol^{-1}	429.38	380.31	375.31
cryst syst	triclinic	monoclinic	monoclinic
space group	*P*2(1)/*c*	*C*2/*c*	*P*2(1)/*c*
unit cell dimens			
a, Å	11.1505(7)	16.2500(5)	14.802(2)
b, Å	11.7696(7)	8.2979(3)	13.4051(19)
c, Å	14.5244(9)	22.6521(7)	15.272(2)
β, deg	105.222(1)	104.620(1)	103.045(2)
cell volume, Å^3	1839.3(2)	2955.53(17)	2952.1(7)
Z	4	6	8
d_{calcd}, g cm^{-3}	1.551	1.709	1.689
abs coeff, mm^{-1}	0.793	0.981	0.977
F(000)	880	1560	1536
cryst size, mm	0.34 × 0.31 × 0.1	0.77 × 0.19 × 0.10	0.60 × 0.22 × 0.07
θ range for data collection, deg	2.26−28.01	2.59−32.56	2.04−25.00
index ranges	$-14 \le h \le 14$, $-14 \le k \le 15$, $-18 \le l \le 18$	$-24 \le h \le 24$, $-12 \le k \le 12$, $-34 \le l \le 34$	$-17 \le h \le 11$, $-15 \le k \le 15$, $-17 \le l \le 18$
reflns collected	21 741	39 288	15 623
independent reflns	4321 [*R*(int) = 0.0435]	5376 [*R*(int) = 0.0818]	5180 [*R*(int) = 0.0710]
completeness to θ (max)	96.9%	99.8%	99.7%
data/restraints/param	4321/0/299	5376/0/255	5180/0/397
GOF on F^2	0.852	0.977	0.952
final *R* indices [$I > 2\sigma(I_0)$]	R1 = 0.0372, wR2 = 0.0688	R1 = 0.0383, wR2 = 0.0871	R1 = 0.0609, wR2 = 0.1412
R indices (all data)	R1 = 0.0604, wR2 = 0.0746	R1 = 0.0516, wR2 = 0.0912	R1 = 0.1130, wR2 = 0.1612
largest diff. peak/hole, e Å^{-3}	0.367/−0.275	0.845/−0.413	0.078/−0.499

[a] Per formula unit.

Experimental Section

Materials. V_2O_5 (Loba Chemie, Mumbai, India), pyridoxal hydrochloride (Hpydx·HCl; Fluka Chemie, GmbH, Buchs, Switzerland), acetyl acetone (Hacac; Aldrich, Milwaukee, WI), salicylaldehyde, and 30% aqueous H_2O_2 (Qualigens, Mumbai, India) were used as obtained. *S*-Benzyldithiocarbazate,[26] *S*-methydithiocarbazate,[27] and [VO(acac)$_2$][28] were prepared according to the methods reported in the literature.

Instrumentation. Elemental analyses of the ligands and complexes were performed by the microanalytical section of the Central Drug Research Institute, Lucknow, India. IR spectra were recorded as KBr pellets on a Perkin-Elmer model 1600 FT-IR spectrometer. Electronic absorption spectra were measured in methanol or dimethylformamide (DMF) with an UV-1601 PC UV−vis spectrophotometer. ^{1}H NMR spectra were obtained on a Bruker 200 spectrometer, ^{13}C and ^{51}V NMR spectra on a Bruker Avance 400 MHz spectrometer at 94.73 MHz, and vials had the common parameter settings. NMR spectra were usually recorded in deuterated dimethyl sulfoxide (DMSO-d_6), and ^{51}V NMR values are quoted relative to $VOCl_3$ as the external standard. Selected ^{51}V NMR results have also been obtained in CD_3OD. Cyclic voltammetric (CV) experiments were carried out in acetonitrile using a platinum working electrode and a Ag−AgCl reference electrode on a Basic Electrochemistry System model ECDA 001 of Con Serve Enterprises, Mumbai, India. Thermogravimetric analyses (TGA) of the complexes were carried out under an oxygen atmosphere using a TG Stanton Redcroft STA 780 instrument.

Crystal Structure Determination. Crystal structure data were collected at 153(2) K on a Bruker SMART Apex CCD diffractometer, using a graphite monochromator and Mo Kα radiation (λ = 0.710 73 Å). Hydrogen atoms were found or placed into calculated positions and included in the last cycles of refinement. Absorption corrections have been carried out with SADABS. The program systems SHELXS 86 and SHELXL 93 were used throughout. Crystal data and details of the data collection and refinement are collated in Table 1. CCDC numbers: **1**, 271678; **3**, 271679; **4**, 271680.

In Vitro Testing against *E. histolytica*. The ligands and their metal complexes were screened in vitro for antiamoebic activity against HM1:1MSS strain of *E. histolytica* by the microdilution method.[29] *E. histolytica* trophozoites were cultured in a TYIS-33 growth medium as described previously in wells of 96-well microtiter plates (Costar).[30] All of the compounds (ca. 1 mg) were dissolved in DMSO (40 μL), and the test solutions were prepared immediately before use by adding enough culture medium to obtain a concentration of 1 mg/mL. Dissolution was facilitated by mild sonication in a sonicleaner bath for a few minutes. As evidenced by a comparison of the UV−vis spectra of the complexes dissolved in DMSO, on the one hand, and DMSO + TYIS-33 medium, on the other hand, the complexes preserve their integrity under these conditions.[31,32] Two-fold serial dilutions were made in the wells in 170 μL of a medium. Each test included MNZ as a standard amoebicidal drug, control wells (culture medium plus amoebae), and a blank (culture medium only). All of the experiments were carried out in triplicate at each concentration level and repeated three times. The control wells were prepared from a confluent culture by pouring off the medium, adding 2 mL of a fresh medium,

(26) Ali, M. A.; Tarafder, M. T. H. *J. Inorg. Nucl. Chem*. **1977**, *39*, 1785−1791.
(27) Das, M.; Livingstone, S. E. *Inorg. Chim. Acta* **1976,** *19*, 5−10.
(28) Row, R. A.; Jones, M. M. *Inorg. Synth*. **1957**, *5*, 113−116.
(29) Wright, C. W.; O'Neill, M. J.; Phillipson, J. D.; Warhurst, D. C. *Antimicrob. Agents Chemother*. **1988**, *32*, 1725−1709.
(30) Diamond, L. S.; Harlow, D. R.; Cunnick, C. C. *Trans. R. Soc. Trop. Med. Hyg*. **1978**, *72*, 431−432.
(31) Gillin, F. D.; Reiner, D. S.; Suffness, M. *Antimicrob. Agents Chemother*. **1982**, *22*, 342−345.
(32) Keene, A. T.; Harris, A.; Phillipson, J. D.; Warhurst, D. C. *Planta Med*. **1986**, 278−285.

and chilling the culture on ice to detach the organism from the flask wall. The number of amoeba per milliliter was estimated with a heamocytometer, and trypan blue exclusion was used to confirm viability. The cell suspension used was diluted to 10^5 organisms/mL by adding a fresh culture medium, and 170 μL of this suspension was added to the test and control wells so that the wells were completely filled (total volume of 340 μL). An inoculum of 1.7×10^4 organisms/well was chosen so that confluent, but not excessive, growth took place in the control wells. The plates were sealed with expanded polystyrene, secured with tape, placed in a modular incubation chamber, and gassed for 10 min with nitrogen before incubation at 37 °C for 72 h.

Assessment of the Antiamoebic Activity. After incubation, the growth of amoebae in the plate was checked with a low-power microscope. The culture medium was removed by inverting the plate and shaking it gently. The plate was then immediately washed once in a sodium chloride solution (0.9%) at 37 °C. This procedure was completed quickly, and the plate was not allowed to cool in order to prevent the detachment of amoebae. The plate was allowed to dry at room temperature, and the amoebae were fixed with methanol and, when dry, stained with 0.5% aqueous eosin for 15 min. The stained plate was washed once with tap water and then twice with distilled water and allowed to dry. A 200-μL portion of a 0.1 M sodium hydroxide solution was added to each well to dissolve the protein and release the dye. The optical density of the resulting solution in each well was determined at 490 nm with a microplate reader. The percent of inhibition of amoebal growth was calculated from the optical densities of the control and test wells and plotted against the logarithm of the dose of the drug tested. Linear regression analysis was used to determine the best-fitting straight line, from which the IC_{50} value was obtained.

Preparation of Ligands. (i) H_2pydx-sbdt (I). A mixture of pyridoxal hydrochloride (1.02 g, 5 mmol) and *S*-benzyldithiocarbazate (0.98 g, 5 mmol) in ca. 50 mL of methanol was refluxed on a water bath for 4 h. After reduction of the volume of the solvent to ca. 30 mL, it was cooled to ambient temperature within 4 h. During this time, a yellow solid of **I** precipitated, which was filtered off, washed with methanol, and dried. Finally, it was recrystallized from methanol to give a fine needlelike crystalline solid. Yield: 1.53 g (88%). Anal. Calcd for $C_{16}H_{17}N_3O_2S_2$ (347.45): C, 55.30; H, 4.90; N, 12.10. Found: C, 55.16; H, 4.73; N, 12.0. Selected IR data (KBr, ν_{max}/cm^{-1}): 3410 (OH), 2750−3080 (NH- - -OH), 1639, 1621 (C═$N_{azomethine}$), 1048 (C═S).

(ii) H_2pydx-smdt (II). This ligand was prepared by following the procedure outlined for **I**. Recrystallization was done from methanol. Yield: 1.15 g (85%). Anal. Calcd for $C_{10}H_{13}N_3O_2S_2$ (271.35): C, 44.28; H, 4.80; N, 15.50. Found: C, 44.1; H, 4.94; N, 15.33. Selected IR data (KBr, ν_{max}/cm^{-1}): 3400 (OH), 2550−3025 (NH- - -OH), 1618 (C═$N_{azomethine}$), 1030 (C═S).

Preparation of Complexes. (i) [VO_2(Hpydx-sbdt)] (1). Method A. Vanadium(V) oxide (0.91 g, 5 mmol) was suspended in aqueous KOH (0.28 g, 5 mmol in 10 mL) and stirred for 2 h with occasional heating at 50 °C. The potassium vanadate solution thus generated was filtered. A filtered solution of **I** (1.74 g, 5 mmol) dissolved in 20 mL of aqueous KOH (0.56 g, 10 mmol) was added to the above solution with stirring. After $^1/_2$ h, the pH of the reaction mixture was slowly adjusted to ca. 7.0 with 4 M HCl. The stirring was continued for 2 h, and the precipitated yellow solid was filtered off, washed with water, and dried in vacuo over silica gel. Upon crystallization from ca. 50 mL of methanol, red crystalline **1** slowly separated out within 2 weeks. This was filtered off, washed with cold methanol, and dried in vacuo over silica gel. Yield: 0.97 g (45%). Anal. Calcd for $C_{16}H_{16}N_3O_4S_2V$ (429.38): C, 44.76; H, 3.76; N, 9.79. Found: C, 44.37; H, 3.88; N, 9.62. Selected IR data (KBr, ν_{max}/cm^{-1}): 3400 (OH), 3125 ($NH_{pyridoxal}$), 1631 (C═$N_{azomethine}$), 780 (C−S), 951, 874 (O═V═O). ^{51}V NMR (DMSO-d_6, δ/ppm): −469.6.

Method B. A solution of **I** (1.74 g, 5 mmol) in methanol (20 mL) was added with stirring to [VO(acac)$_2$] (1.33 g, 5 mmol) dissolved in methanol (10 mL), and the resulting reaction mixture was refluxed on a water bath for 8 h. After cooling to room temperature, KOH (0.28 g, 5 mmol) was added, and the brown suspension was oxidized by passing air through the solution overnight, resulting in a gradual conversion of the suspension to a red solution. This was filtered, and the clear solution was kept at ca. 10 °C for several days. The red crystals that separated were filtered off, washed with cold methanol, and dried in vacuo over silica gel. Yield: 0.75 g (35%). Analytical and spectral data of the isolated complex matched well with that of **1** prepared according to method A.

(ii) [{VO(pydx-sbdt)}$_2\mu$-O]·2H_2O (2·2H_2O). A solution of **1** (0.429 g, 1 mmol) in 20 mL of methanol was heated on a water bath for 20 min to yield a blackish solid, which slowly separated out. After cooling of the reaction flask to room temperature, the isolated solid was filtered off, washed with methanol, and dried in vacuo over silica gel. Yield: 0.36 g (85%). Anal. Calcd for $C_{32}H_{34}N_6O_9S_4V_2$ (876.78): C, 43.84; H, 3.88; N, 9.58; S, 14.60. Found: C, 43.54; H, 3.92; N, 9.57; S, 14.44. Selected IR data (KBr, ν_{max}/cm^{-1}): 3410 (OH), 1622 (C═$N_{azomethine}$), 770 (C−S), 980 (V═O), 865 [V−(μ-O)−V]. ^{51}V NMR (DMSO-d_6, δ/ppm): −472.74.

(iii) [VO_2(Hpydx-smdt)]·1.5H_2O (3·1.5H_2O). To a solution of **II** (1.02 g, 5 mmol) in 15 mL of methanol was added K_2CO_3 (0.67 g, 5 mmol) dissolved in 5 mL of water, and the solution filtered. A solution of [VO(acac)$_2$] (1.33 g, 5 mmol) in 15 mL of methanol was added, and the reaction mixture was refluxed for 1 h to give a green suspension. This was subjected to aerial oxidation for 2 days with occasional shaking. During this process, the green suspension slowly disappeared, and the color changed to red-brown. After the suspension was filtered and kept at ca. 10 °C, red-brown crystals of **3** separated within 3−5 days. These were filtered off, washed with cold methanol, and dried in vacuo over silica gel. Yield: 0.98 g (55%). Anal. Calcd for $C_{10}H_{15}N_3O_{5.5}S_2V$ (380.31): C, 31.59; H, 3.88; N, 11.06; S, 16.83. Found: C, 31.23; H, 3.82; N, 10.88; S, 16.57. Selected IR data (KBr, ν_{max}/cm^{-1}): 3400 (OH), 1593 (C═$N_{azomethine}$), 707 (C−S), 947, 865 (O═V═O). ^{51}V NMR (DMSO-d_6, δ/ppm): −468.96.

Impure **3** can also be prepared from KVO_3 and **II** by the method A outlined for **1**.

(iv) [{VO(pydx-smdt)}$_2\mu$-O]·2CH_3OH (4·2CH_3OH). This complex was prepared as outlined for **2** using 1 mmol of **3** in 20 mL of methanol. Yield: 0.55 g (74%). Anal. Calcd for $C_{22}H_{30}N_6O_9S_4V_2$ (752.64): C, 35.11; H, 4.02; N, 11.17; S, 17.01. Found: C, 35.0; H, 4.18; N, 11.06; S, 17.24. Selected IR data (KBr, ν_{max}/cm^{-1}): 3300 (OH), 1621 (C═$N_{azomethine}$), 752 (C−S), 947, 986 (V═O), 855 [V−(μ-O)−V]. ^{51}V NMR (DMSO-d_6, δ/ppm): −468.55.

Results and Discussion

Synthesis, Reactivity, and Solid-State Characteristics. The structures of the vanadium(V) complexes characterized on the basis of elemental and electrochemical analyses, spectroscopic (IR, UV−vis, and ^{1}H, ^{13}C, and ^{51}V NMR) data, TGA studies, and the X-ray diffraction analyses of **1**, **2**, and **4** are shown in Chart 1.

Reaction between equimolar methanolic solutions of [VO(acac)$_2$] and the ligands **I** or **II** in the presence of KOH/K_2-

Chart 1

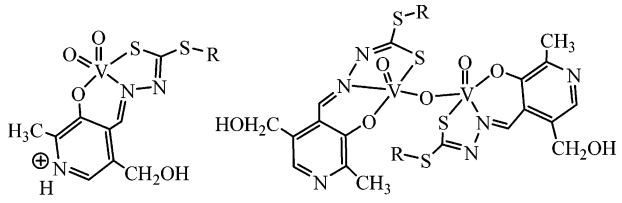

R = CH_2Ph: **1**
R = CH_3: **3**

R = CH_2Ph: **2**
R = CH_3: **4**

CO_3, followed by aerial oxidation, resulted in the formation of the neutral, red-brown dioxovanadium(V) complexes **1** and **3**, devoid of any paramagnetic impurities (electron paramagnetic resonance and NMR evidence). Equations 1 and 2 represent the synthetic procedures.

$$[VO(acac)_2] + K_2\text{pydx-sbdt} \rightarrow [V^{IV}O(\text{pydx-sbdt})] + 2\text{acacK} \quad (1)$$

$$2[V^{IV}O(\text{pydx-sbdt})] + H_2O + \frac{1}{2}O_2 \rightarrow \underset{\mathbf{1}}{2[V^{V}O_2(\text{Hpydx-sbdt})]} \quad (2)$$

Complex **1** has also been obtained from the reaction of potassium vanadate, generated in situ by dissolving V_2O_5 in aqueous KOH, with the potassium salt of **I** at pH ca. 7.0, while the corresponding reaction with ligand **II** produced **3** in poor quality only. Methanolic solutions of **1** and **3** are, although very stable at ambient temperature, yield the blackish binuclear μ-oxo complexes **2** and **4** on heating (eq 3).

$$2[V^{V}O_2(\text{Hpydx-sbdt})] \rightarrow \underset{\mathbf{2}}{[\{V^{V}O(\text{pydx-sbdt})\}_2\mu\text{-O}]} + H_2O \quad (3)$$

The ligands coordinate out of their dianoic [ONS(2−)] thioenolate tautomeric form (cf. Scheme 1, right). Complexes **1**−**4** are soluble in DMSO and DMF; **1** and **3** are additionally soluble in methanol and ethanol.

Structure Description. ORTEP plots of the dioxo complexes **1** and **3** along with the atom numbering schemes are shown in Figure 1. Complex **3** crystallizes with 1.5 water of crystallization per formula unit (six H_2O per four formula units). Table 2 contains selected bond lengths and angles. The coordination geometry of the five-coordinated vanadium complexes can be described as slightly distorted ($\tau = 0.13$ and 0.11) tetragonal-pyramidal with one of the doubly bonded oxygen atoms in the apex. The imine nitrogen, phenolate oxygen, and thioenolate sulfur of the dibasic tridentate ligand and one of the oxygens of the dioxo group form the tetragonal plane. The distortion is significantly less than that in the related thiohydrazonato complexes [VO(OEt)(sal-sbdt)] (H_2sal-sbdt = Schiff base derived from salicylaldehyde and *S*-benzyldithiocarbazate; $\tau = 0.27$)[23i] and [VO_2(acpy-sbdt)] (Hacpy = Schiff base derived from acetylpyridine and *S*-benzyldithiocarbazate; $\tau = 0.47$)[23h] The vanadium atom is displaced from the tetragonal plane toward the apex by 0.809 Å. The bond lengths d(V−N_2) are comparatively long as a consequence of the trans effect by the equatorial oxo group. The bond distance d(V−O_{eq}) = 1.6607(11) Å in **3** is significantly longer than the other, about normal (see also **4**) V═O bonds in **1** and **3**, a fact reflects the more intimate involvement of the equatorial oxo group of **3** in intermolecular hydrogen bonding [to water OW(1) and the alcoholic function on the pyridoxal moiety; cf. Table 2]. The protonated pyridine nitrogen is engaged in hydrogen bonds to O(1) of **1** and OW(2) of **3**.

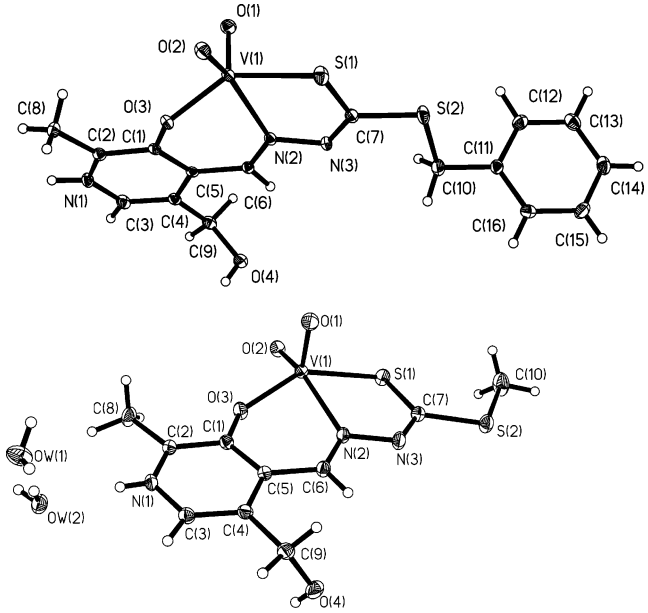

Figure 1. ORTEP plots (30% probability level) of **1** (top) and **3**·1.5H_2O (bottom).

The ORTEP plot of the dinuclear complex **4** is shown in Figure 2. Selected structural parameters are collected in Table 3. The geometry of each unit is similar to those found in **1** and **3**. The ONS donor set of the dibasic tridentate ligand and the bridging oxygen O(1) form the tetragonal plane. The distances d(V(1)−O(11)) = 1.585(4) Å and d(V(2)−O(21)) = 1.579(4) Å are well within the expected range. These terminal oxygen atoms are in the syn orientation, with a torsion angle of almost 0°. Anti orientations of the V═O moieties in the {VOL}$_2\mu$-O core have been reported for H_2L = dihydroxyazobenzene[33] and aroylhydrazones of salicylaldehydes,[34] intermediate orientations for Schiff base ligands containing salicylaldehydes and amino acids such as serine (torsion angles 11.6°[35a] and 106.6°[35b]) and alanine (torsion angle 83.7°[35c]). Similarly, the ligand oxygen and sulfur functions in the halves of the dinuclear complexes may be syn (cis) or anti (trans) oriented. In the present example, complex **4**, the anti orientation is realized. The azomethine nitrogen lies trans to the bridging oxygen. The d(V−N) values in **4** [2.130 and 2.123(5) Å] thus are significantly

(33) Dutta, S.; Basu, P.; Chakravorty, A. *Inorg. Chem.* **1993**, *32*, 5343−5348.
(34) Sangeetha, N. R.; Pal, S. *Bull. Chem. Soc. Jpn.* **2000**, *73*, 357−363.
(35) (a) Pessoa, J. C.; Silva, J. A. L.; Vieira, A. L.; Vilas-Boas, L.; O'Brien, P.; Thornton, V. *J. Chem. Soc., Dalton Trans.* **1992**, 1745−1749. (b) Grüning, C.; Schmidt, H.; Rehder, D. *Inorg. Chem. Commun.* **1999**, *2*, 57−59. (c) Mondal, S.; Ghosh, P.; Chakravorty, A. *Inorg. Chem.* **1997**, *36*, 59−63.

Table 2. Selected Bond Lengths (Å) and Angles (deg) for **1** and **3**

	bond length (Å)			bond angle (deg)	
	1	**3**		**1**	**3**
V−O(1)	1.6255(15)	1.6607(11)	O(1)−V−O(2)	109.80(8)	107.84(6)
V−O(2)	1.6292(15)	1.6057(11)	O(2)−V−O(3)	108.30(7)	108.66(5)
V−O(3)	1.9037(14)	1.9054(11)	O(2)−V−N(2)	149.98(8)	151.16(5)
V−N(2)	2.2203(17)	2.2055(13)	O(1)−V−S(1)	105.67(6)	102.55(4)
V−S(1)	2.3642(7)	2.3902(5)	O(2)−V−S(1)	89.18(6)	88.36(4)
N(2)−N(3)	1.405(2)	1.3957(17)	O(3)−V−N(2)	80.85(6)	81.41(5)
C(7)−S(1)	1.733(2)	1.7285(16)	O(3)−V−S(1)	141.92(5)	144.40(4)
C(7)−S(2)	1.743(2)	1.7543(16)	N(2)−V−S(1)	76.99(5)	76.87(3)
C(6)−N(2)	1.301(3)	1.299(2)			
H bonds	O(1)···N(1), 2.679	O(1)···OW(1), 2.866	∠C(6) (ave)	120.0	120.0
	O(2)···O(4), 2.945	O(1)···O(4), 2.945	∠N(2) (ave)	119.7	119.8
		N(1)···OW(2), 2.673	∠C(7) (ave)	120.0	120.0
		O(4)···OW(2), 2.786			
		OW(1)···OW(2), 2.808			

Table 3. Selected Bond Lengths (Å) and Bond Angles (deg) for **4**

V(1)−O(1)	1.771(4)	V(2)−O(1)	1.809(4)	V(1)−O(1)−V(2)	167.9(3)		
V(1)−O(11)	1.585(4)	V(2)−O(21)	1.579(4)	O(1)−V(1)−O(11)	107.6(2)	O(21)−V(2)−O(1)	107.6(2)
V(1)−O(12)	1.888(4)	V(2)−O(22)	1.906(4)	O(11)−V(1)−O(12)	111.1(2)	O(21)−V(2)−O(22)	112.2(2)
V(1)−N(11)	2.130(5)	V(2)−N(21)	2.123(5)	O(1)−V(1)−O(12)	93.89(18)	O(1)−V(2)−O(22)	92.42(17)
V(1)−S(11)	2.342(2)	V(2)−S(21)	2.341(2)	O(11)−V(1)−N(11)	96.7(2)	O(21)−V(2)−N(21)	97.5(2)
S(11)−C(10)	1.742(6)	S(21)−C(30)	1.725(6)	O(1)−V(1)−N(11)	154.6(2)	O(1)−V(2)−N(21)	154.0(2)
S(12)−C(10)	1.735(6)	S(22)−C(30)	1.764(6)	O(12)−V(1)−N(11)	83.78(17)	O(22)−V(2)−N(21)	83.95(17)
N(11)−C(9)	1.299(7)	N(21)−C(29)	1.297(7)	O(11)−V(1)−S(11)	108.43(15)	O(21)−V(2)−S(21)	108.06(16)
N(11)−N(12)	1.395(6)	N(21)−N(22)	1.393(6)	O(1)−V(1)−S(11)	86.82(14)	O(1)−V(2)−S(21)	86.54(14))
N(12)−C(10)	1.292(7)	N(22)−C(30)	1.299(7)	O(12)−V(1)−S(11)	138.13(15)	O(22)−V(2)−S(21)	138.01(14)
				N(11)−V(1)−S(11)	78.49(13)	N(21)−V(2)−S(21)	79.30(14)

shorter than those in **1** [2.2203(17) Å] and **3** [2.2055(13) Å]. Angles at the bridging oxygen may span the range from 107 to 180°; in **4**, the angle V(1)−O(1)−V(2) amounts to 167.9(3)°. Intermolecular hydrogen bonds are formed between the methanols of crystallization and the pyridoxal nitrogens, d(N(13)···O(100)) = 2.779 Å and d(N(23)···O(200)) = 2.757 Å, and between the alcoholic pyridoxal functions and the noncoordinated hydrazone nitrogens, d(N(12)···O(23)) = 2.872 Å and d(N(22)···O(13)) = 2.891 Å.

TGA Studies. The TGA profiles of the complexes show that **1** is stable up to 180 °C, while the other three complexes lose weight exothermically in the temperature range of 100−160 °C, corresponding to the loss of water or methanol associated with them. The solvent-free species, in general, decompose in three steps. For **2**, the first weight loss (17.7%) takes place in the narrow temperature range of 240−260 °C, followed by a mass loss of 20.78% in a broader temperature range (260−390 °C). The third step starts at 360 °C and ends at 460 °C, with a mass loss of 40.3%. The total mass loss of 78.8% corresponds to the loss of all organic components (calcd mass loss: 78.8%). The remaining residue of 19.15% slowly gains weight and stabilizes at 700 °C with 19.75%, equivalent to the formation of V_2O_5 (calcd: 20.53%). The complexes **3** and **4** exhibit decomposition patterns similar to that of **2** and yield V_2O_5 as the final product.

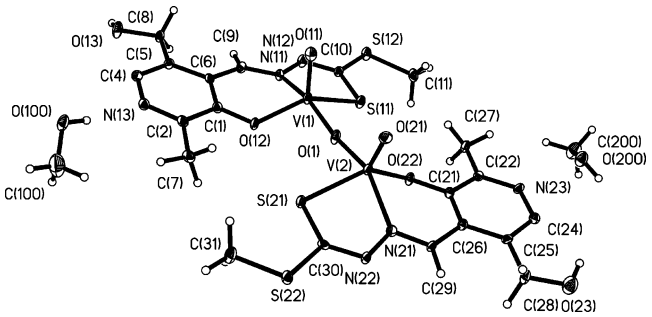

Figure 2. ORTEP plots (30% probability level) of **4**·2CH_3OH.

IR Spectra. IR spectrum of the ligand **I** exhibits a broad feature between 2750 and 3080 cm^{-1} and a sharp band at 1048 cm^{-1}, due to hydrogen-bonded ν(NH) and the ν(C═S) stretch, respectively; the corresponding bands for **II** are between 2550 and 3025 cm^{-1} and at 1030 cm^{-1}. The appearance of both of these bands in the ligands indicates their thiocarbonyl nature (cf. Scheme 1, left) in the solid state. This is further supported by the absence of an IR band at ca. 2500 cm^{-1} for ν(SH). The disappearance of these bands upon complex formation suggests the breaking of hydrogen bonds and thioenolization of the C═S group (Scheme 1, right), followed by coordination of the thioenolate sulfur to vanadium after deprotonation. The coordination through the tautomeric enthiol form of the ligand [−N═C(SH)− functionality] after deprotonation is commonly observed in comparable complexes[23] and is further corroborated by the appearance of a new band in the range of 710−770 cm^{-1}, characteristic of the ν(C−S) stretch. A strong ligand band at 1639 cm^{-1} (in **I**) and at 1618 cm^{-1} (in **II**) was assigned to ν(C═$N_{azomethine}$), and this band shifts to lower wavenumber by 8−25 cm^{-1} in the complexes, thereby indicating the participation of the azomethine nitrogen atom in coordination. The band belonging to the coordinated phenolate oxygen could not be assigned unequivocally because of the strong absorption of ν(OH) of the alcoholic group in the 3400-cm^{-1} region.

Table 4. Electronic Spectral Data of Ligands and Complexes

compound	λ_{max}/nm (ϵ/M^{-1} cm^{-1})
I	211 (20 417), 337 (13 999), 360 (14 148)
1	215 (23 118), 302 (11 340), 416 (3711)
2	291 (18 898), 356 (10 558), 412 (9320)
II	209 (19 088), 335 (15 736), 355 (15 010)
3	222 (16 393), 309 (9966), 420 (2668)
4	295 (16 667), 358 (9043), 410 (7740)

The neutral dioxo complexes display two sharp bands at 951 and 874 cm^{-1} (in **1**) or 947 and 865 cm^{-1} (in **3**), corresponding to the $\nu_{antisym}(VO_2)$ and $\nu_{sym}(VO_2)$ modes. The lowering of $\nu_{sym}(VO_2)$ is possibly due to the involvement of one of the oxygens in hydrogen bonding with other groups present in the complexes (vide supra). The dinuclear complexes exhibit a sharp band at ca. 980 cm^{-1} due to ν-(V═O) and a broad but medium intensity band at ca. 860 cm^{-1} due to the ν[V−(μ-O)−V] mode.

Electronic Spectra. The UV spectra (Table 4) of both of the ligands recorded in methanol exhibit three bands at 211, 337, and 360 nm (**I**) and 209, 335 and 355 nm (**II**). The most probable assignments of these bands are $\varphi \rightarrow \varphi^*$, $\pi \rightarrow \pi^*$, and n $\rightarrow \pi^*$ transitions, respectively. A weak shoulder at ca. 309 nm is assignable to hydrogen bonding; in DMF, the 309-nm band is no longer present. The neutral complexes exhibit only two ligand bands at ca. 215 and 305 nm (mononuclear complexes) and at ca. 295 and 358 nm (dinuclear complexes). In addition, there is a band with a low extinction coefficient in the visible region at ca. 415 nm, which is assigned to a ligand-to-metal charge transfer from the phenolate oxygen to an empty d orbital of the vanadium ion. Because vanadium(V) complexes have a $3d^0$ configuration, d−d bands are not expected.

^{1}H, ^{13}C, and ^{51}V NMR Spectra. ^{1}H NMR spectra of the ligands and complexes were recorded to confirm the coordinating modes of the ligands and are presented in Table 5. Generally, the dinuclear complexes give rise to comparatively broad signals for all of the protons, indicating that the halves of the molecule and thus the coordinated ligands are slightly inequivalent also in solution.

Both ligands show a broad signal at ca. 13.90 ppm due to phenolic OH. The absence of a resonance for NH suggests a predominance of the thioenol tautomer in solution. The absence of both of these signals in the complexes is in accord with the coordination of phenolate oxygen and thiolate sulfur

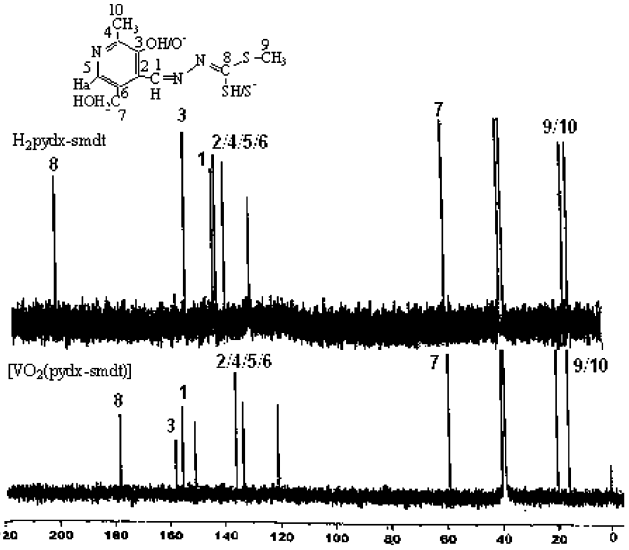

Figure 3. 90.56-MHz $^{13}C\{^1H\}$ NMR spectra (δ in ppm) of **I** (top) and **3** (bottom).

to vanadium. A significant downfield shift of the azomethine (−CH═N−) proton signal in the complexes with respect to the free ligands ($\Delta\delta$ = 0.44−0.50 ppm) is a consequence of the coordination of the azomethine nitrogen. The ^{1}H NMR data are thus consistent with the ONS dibasic tridentate binding mode of the ligands. The monomeric complexes **1** and **3** exhibit a weak and broad (unresolved) band at ca. δ = 5.78, which we tentatively assign to the NH proton of the protonated pyridoxal residue. The hydroxyl proton also appears as an unresolved signal at 3.82 ppm (in **I**) and 3.7 ppm (in **II**). A singlet at 4.9 ppm represents the CH_2 protons of the CH_2OH groups; coupling to the hydroxyl proton apparently is suppressed by exchange of the latter. These features are maintained in the complexes. Other resonances of the ligands appear well within the expected range and do not shift significantly upon complexation.

^{13}C NMR spectra of **I** and **3** have also been recorded and are reproduced in Figure 3. Assignments of the peaks are similar to those reported earlier.[23h] A large positive coordination-induced shift $\Delta\delta = \delta$(complex) − δ(free ligand) of 14 ppm for the azomethine carbon signal conforms to the coordination of this nitrogen function to the vanadium.[36] Similarly, the carbon atoms associated with the C═S and

Table 5. ^{1}H NMR Chemical Shifts

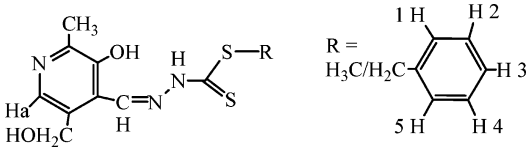

compound[a]	−OH	−OH of CH_2OH	−CH═N−	$-CH_2-$	$-CH_3$	Ha, H1/H5, H2/H4, H3
I	13.90 (b)	3.82 (b)	8.80 (s)	4.49 (s), 4.80 (s)	2.53 (s)	8.20 (s), 7.4 (d), 7.30 (t), 7.2 (dd)
1		3.39 (b)	9.30 (s)	4.85 (s), 4.88 (s)	2.55 (s)	8.05 (s), 7.46 (d), 7.34 (t), 7.27 (dd)
2		3.37 (b)	9.35 (b)	4.48 (b), 4.80 (b)	2.51 (s)	7.20−7.80 (b)
II	13.93 (b)	3.76 (b)	8.85 (s)	4.85 (s)	2.50 (s), 2.60 (s)	8.24 (s)
3		3.39 (b)	9.29 (s)	4.87 (s)	2.49 (s), 2.51 (s)	8.06 (s)
4		3.39 (b)	9.32 (b)	4.83 (b)	2.48 (b), 2.51 (b)	7.98 (b)

[a] Letters given in parentheses indicate the signal structure: s = singlet, d = doublet, t = triplet, dd = doublet of doublets, b = broad (unresolved).

phenolic OH groups also are subjected to large $\Delta\delta$, indicating the involvement of the corresponding functions in coordination.

The $\delta(^{51}V)$ values of the complexes (see also the Experimental Section) display one strong resonance between −468.55 and −472.74 ppm in DMSO-d_6, an expected value for vanadium(V) complexes where a soft S atom participates in coordination in addition to the O and N donor atoms.[37] The resonances are somewhat broadened as a result of quadrupolar interaction (^{51}V, nuclear spin = $^7/_2$; quardrupole moment, −5 fm^2); the line widths at half-height are around 200 Hz, which is still considered to be comparatively narrow in ^{51}V NMR spectroscopy.[38]

Electrochemical Studies. The CVs of **1** and **3** were recorded in the potential range of −1.5 to +0.5 V in acetonitrile (dried over molecular sieves), using 0.1 M tetrabutylammonium tetrafluoroborate as a supporting electrolyte. Both of the complexes exhibit a relatively sharp reduction peak (E_{pc} = −1.173 V for **1** and −1.066 V for **3**), which is indicative of a kinetically facile reduction of vanadium(V) to vanadium(IV). However, a weak oxidation peak (E_{pa} = 0.050 V for **1** and 0.058 V for **3**) and a relatively large peak-to-peak separation suggest that the V^V-V^{IV} redox process is irreversible.[39] Comparable electrochemical data (i.e., reductive and oxidative peak potentials) indicate that the $-SCH_2C_6H_5$ or $-SCH_3$ group has no influence on the vanadium nucleus in these complexes. We have also recorded the CVs of **1** at three different scan rates (50, 100, and 200 mV/s). The oxidation peak in all of the CVs is very weak, and within the complex, the reductive peak potential becomes more negative upon an increase of the scan rate (E_{pc} = −1.156, −1.173, and −1.195 V, respectively), which is further indicative of the irreversible behavior of the complex.

Reactivity toward H_2O_2. The poor stability of the peroxo complexes at ambient temperature in the solid state did not allow isolation and characterization in detail. The formation of peroxo complexes from the corresponding dioxo species was, however, established in a methanolic solution. In a typical experiment, 10 mL of a ca. 1×10^{-4} M solution of **3** was treated with two 1-drop portions of 30% H_2O_2. The reaction, as monitored by electronic absorption spectroscopy (Figure 4), results in a gradual shift of the 420- and 309-nm bands of **3** to 446 and 326 nm, with a marginal decrease in intensity. At the same time, the band appearing at 222 nm drastically decreases in intensity and finally disappears. The amount of peroxo species formation depends on the amount of H_2O_2 added. A similar spectral pattern was also observed for **1**, with a shift of the bands at 416 and 302 nm to 454 and 320 nm and a gradual disappearance of the 215-nm band.

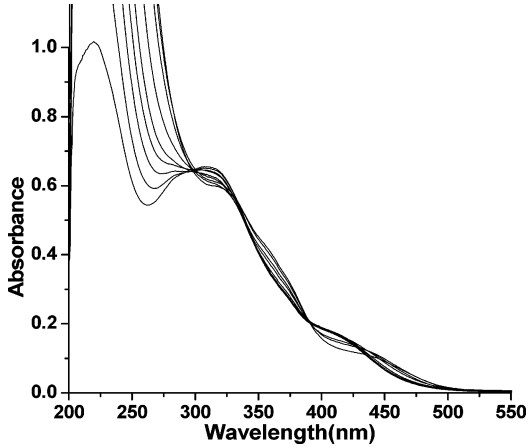

Figure 4. Titration of **3** with 30% H_2O_2. The spectra were recorded after successive additions of 2-drop portions of H_2O_2 to 10 mL of a ca. 0.5×10^{-4} M solution of **3** in MeOH.

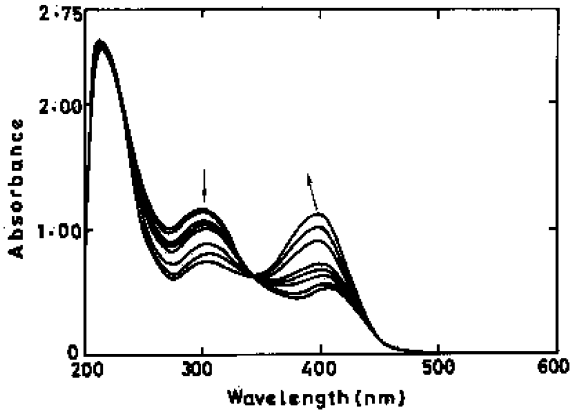

Figure 5. Titration of **1** with KOH dissolved in MeOH. The spectra were recorded after the addition of 1-drop portions of KOH−MeOH to 10 mL of a ca. 10^{-4} M solution of **1** in MeOH.

These spectral changes are consistent with the formation of oxoperoxo complexes $[VO(O_2)(HL)]$ in solution.[40]

Reactivity with KOH and HCl. The reaction of **1** with KOH was monitored by electronic absorption spectroscopy. In a typical reaction, a methanolic solution of **1** (10 mL of ca. 10^{-4} M) was treated with 1-drop portions of dilute (ca. 10^{-2} M) KOH dissolved in methanol. As shown in Figure 5, a progressive increase of the 416-nm band together with a marginal hypsochromic shift to 399 nm was observed, while the 302-nm band only decreased in intensity. The spectral patterns can be restored by neutralization with HCl. We interpret these changes by formation of the potassium salt $K[VO_2(pydx\text{-}sbdt)]$ from the neutral dioxo complex **1** upon loss of the proton attached to the nitrogen of the pyridoxal under alkaline conditions and by reprotonation by the addition of acid. Efforts to isolate $K[VO_2(pydx\text{-}sbdt)]$ always ended up with the neutral complex **1**, although similar dioxovanadium(V) complexes such as $K(H_2O)][VO_2(sal\text{-}sbdt)]$ (where H_2sal-sbdt = Schiff bases derived from salicylaldehyde and *S*-benzyldithiocarbazate)[23h] and $K(H_2O)_2]$-$[VO_2(pydx\text{-}inh)]$ (where H_2pydx-inh = Schiff base derived

(36) Keramidas, A. D.; Papaioannou, A. B.; Vlahos, A.; Kabanos, T. A.; Bonas, G.; Makriyannis, A.; Rapropoulou, C. P.; Terzis, A. *Inorg. Chem.* **1996**, *35*, 357−367.
(37) Rehder, D.; Weidemann, C.; Duch, A.; Priebsch, W. *Inorg. Chem.* **1988**, *27*, 584−587.
(38) Rehder, D. In *Transition Metal Nuclear Magnetic Resonance*; Pregosin, P. S., Ed.; Elsevier: New York, 1991; pp 1−58.
(39) (a) Cavaco, I.; Pessoa, J. C.; Costa, D.; Duarte, M. T.; Gillard, R. D.; Matias, P. *J. Chem. Soc., Dalton Trans.* **1994**, 149−157. (b) Asgedom, G.; Sreedhara, A.; Kivikoski, J.; Valkonen, J.; Rao, C. P. *J. Chem. Soc., Dalton Trans.* **1995**, 2459−2466.
(40) Maurya, M. R.; Khurana, S.; Schulzke, C.; Rehder, D. *Eur. J. Inorg. Chem.* **2001**, 779−788.

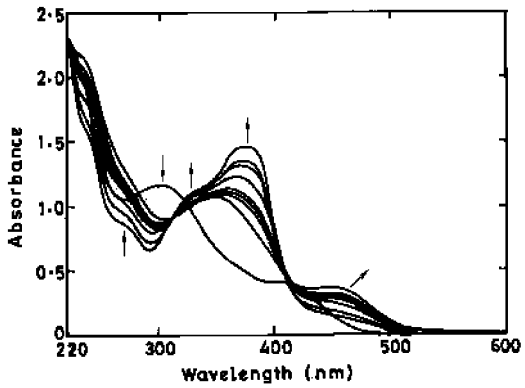

Figure 6. Titration of **1** with a saturated solution of HCl in MeOH. The spectra were recorded after the addition of 1-drop portions of MeOH−HCl to 10 mL of a ca. 10^{-4} M solution of **1** in MeOH.

Scheme 2

$$[VO_2(pydx\text{-}sbdt)]^- \underset{OH^-}{\overset{H^+}{\rightleftharpoons}} [VO_2(Hpydx\text{-}sbdt)] \quad (\mathbf{1}) \quad \underset{OH^-}{\overset{H^+}{\rightleftharpoons}} [VO_2(H_2pydx\text{-}sbdt)]^+$$

$$OH^- \rightleftharpoons H^+$$

$$[VO(OH)(H_2pydx\text{-}sbdt)]^{2+}$$

from pyridoxal and isonicotinic acid hydrazide)[41] are known and have been structurally characterized.

The reactivity of **1** with HCl was also monitored, where **1** (ca. 10^{-4} M solution in methanol) was treated with a 1-drop portion of methanol saturated with HCl gas. The addition of the first 2 drops of a HCl solution results in the merging of the 416- and 302-nm bands to give a broad band at ca. 353 nm. In addition, a new band at 460 nm appears. The further addition of a HCl solution causes a gradual shift of the 353-nm band to 380 nm, along with an increase in the intensity (Figure 6). At the same time, two weak shoulders at ca. 352 and ca. 270 nm slowly appear and later sharpen. Corresponding results have also been obtained with $HClO_4$.

These results possibly reflect the formation of oxohydroxo complexes of composition $[VO(OH)(\mathbf{I})]^{2+}$ via $[VO_2(\mathbf{I})]^+$, with one of the =N−N= nitrogens being the site of protonation upon acidification. Protonation of the hydrazone nitrogen has, e.g., been reported for the structurally characterized complex [VO(Hsal-bhz)] (H_2sal-bhz derives from salicylaldehyde and benzoylhydrazide), which forms upon treatment of the corresponding anionic dioxo complex with HCl.[42] The possible species generated at the various stages of KOH/HCl addition may thus be formulated as shown in Scheme 2.

Upon the addition of a methanolic solution of KOH to $[VO(OH)(\mathbf{I})]^{2+}$, the solution acquired the original spectrum of **1**; the reaction is thus reversible. This reversibility is an important observation in the context of the active site structure and the catalytic activity of vanadate-dependent haloperoxidases, for which a hydroxo ligand at the vanadium center has been made plausible on the basis of X-ray diffraction data.[18e,43] Oxohydroxovanadium complexes have previously been generated upon acidification of $[K(H_2O)_2][VO_2(pydx\text{-}inh)]$[41] and $[K(H_2O)_2][VO_2(Clsal\text{-}sbdt)]$[23h] ($H_2$-Clsal-sbdt = ligand derived from 5-chlorosalicylaldehyde and *S*-benzyldithiocarbazate). An oxohydroxo complex, $[VO(OH)(LH)]^+$ {where LH = *N*-[(*o*-hydroxyphenyl)methyl]-*N*′-(2-hydroxyethyl)ethylenediamine},[44] has been reported to form from a dinuclear dioxovanadium(V) precursor in a similar manner. $[V^VO(OH)(8\text{-oxyquinolinate})_2]$[45] and $[V^{IV}O(OH)Tp(H_2O)]$ [Tp = tris(3,5-diisopropyl-1-pyrazolyl)borate-(1−)][46] have been characterized in the solid state.

Table 6. In Vitro Screening for Amoebicidal Activity of the Ligands and Their Vanadium Complexes against HM1:1MS Strain of *E. Histolytica*

compound	IC_{50} (μM)	stand dev
I	9.45	0.02
1	1.64	0.05
2	1.25	0.02
II	11.05	0.11
3	2.08	0.07
4	1.67	0.12
$[VO(acac)_2]$	6.88	0.05
MNZ	1.89	0.04

Antiamoebic Activity. The ligands and their dioxo- and oxovanadium(V) complexes were screened for antiamoebic activity in vitro using HM1:IMSS strain of *E. histolytica*. The 50% inhibition concentration (IC_{50}) values of ligands and their complexes in micromolars are indexed in Table 6. MNZ was used as the reference drug (IC_{50} = 1.89 μM). The free ligands derived from *S*-benzyldithiocarbazate (**I**) and *S*-methyldithiocarbazate (**II**) exhibited antiamoebic activity with IC_{50} values of 9.45 and 11.05 μM, respectively. A comparison of these values with that of MNZ suggests that the ligands do not exhibit ameobicidal activity. The complexes **1** and **2** derived from the ligand *S*-benzyldithiocarbazate, and **4** derived from *S*-methyldithiocarbazate, showed slightly better antiamoebic activity (**1**, IC_{50} = 1.64 μM; **2**, IC_{50} = 1.25 μM; **4**, IC_{50} = 1.67 μM) than the reference drug MNZ (IC_{50} = 1.89 μM). The high activity of the complexes as compared to the ligands showed that complexation of the organic ligand to vanadium substantially enhances the activity. A possible explanation is that, by coordination, the polarities of the ligand and the central metal ion are reduced through charge equilibration, which favors permeation of the complexes through the lipid layer of the cell membrane.[47] The IC_{50} value for the vanadium precursor $[VO(acac)_2]$ was also determined, establishing that the precursor has no activity against *E. histolytica*. The significance of the statistical difference between the IC_{50} values of MNZ and the most active compounds **1**, **2**, and **4** was evaluated by the *T* test. The values of the calculated *T* were found to be higher than the table value of *T* at the 5% level, thus demonstrating that the complexes under study should significantly improve

(41) Maurya, M. R.; Agarwal, S.; Bader, C.; Rehder, D. *Eur. J. Inorg. Chem.* **2005**, 147−157.
(42) Plass, W.; Pohlmann, A.; Yozgatli, H. K. *J. Inorg. Biochem.* **2000**, *80*, 181−183.
(43) Macedo-Ribeiro, S.; Hemrika, W.; Renirie, R.; Wever, R.; Messerschmidt, A. *J. Biol. Inorg. Chem.* **1999**, *4*, 209−219.
(44) Colpas, G. J.; Hamstra, B. J.; Kampf, J. W.; Pecoraro, V. L. *Inorg. Chem.* **1994**, *33*, 4669−4675.
(45) Giacomelli, A.; Floriani, C.; De Souza Duarte, A. O.; Chiesi-Villa, A.; Guastino, C. *Inorg. Chem.* **1982**, *21*, 3310−3316.
(46) Kosugi, M.; Hikichi, S.; Akita, V.; Moro-oka, Y. *Inorg. Chem.* **1999**, *38*, 2567−2578.
(47) Ramadan, A. M. *J. Inorg. Biochem.* **1997**, *65*, 183−189.

the treatment of amoebiasis. The oxo-bridged binuclear complex **2** is the most active of the vanadium series.

Conclusions

Two new neutral dioxovanadium(V) complexes **1** and **3**, having ONS donor sets derived from pyridoxal and *S*-benzyldithiocarbazate or *S*-methylditiocarbazate, have been prepared and characterized. Ring nitrogen of the pyridoxal moiety exists in the protonated form in these complexes. These complexes model part of the structure of the active site of the vanadate-dependent haloperoxidases. The formation of intermediates proposed for the catalytic cycle of haloperoxidases, i.e., oxohydroxo species $[VO(OH)]^{2+}$ and oxoperoxo species $[VO(O_2)]^{+}$, has also been made plausible on the basis of characteristic changes observed by UV−vis spectroscopy in solutions of these complexes treated with HCl and hydrogen peroxide, respectively. The complexes **1** and **2** can be converted into its potassium salt (characterized in solution) or oxo-bridged binuclear complexes **2** and **4**. The complexes exhibit in vitro antiamoebic activity toward *E. histolytica* better than MNZ, a medication commonly used in amoebiasis.

Acknowledgment. M.R.M. and A.K. thank the Council of Scientific and Industrial Research, New Delhi, India (Grant 01(1826)/02/EMR-II), for financial assistance. We also acknowledge C, H, N, and S analyses carried out by SAIC, Central Drug Research Institute, Lucknow, India.

IC050811+